Information Rate Optimization for the Non-Regenerative Linear MIMO Relay Channel with a Direct Link and Variable Duty Cycle

Original
Information Rate Optimization for the Non-Regenerative Linear MIMO Relay Channel with a Direct Link and Variable Duty Cycle / Taricco, G.. - In: IEEE TRANSACTIONS ON INFORMATION THEORY. - ISSN 0018-9448. - STAMPA. - 68:9(2022), pp. 5889-5900. [10.1109/TIT.2022.3166073]

Availability:
This version is available at: 11583/2971014 since: 2022-09-06T16:13:44Z

Publisher:
Institute of Electrical and Electronics Engineers Inc.

Published
DOI:10.1109/TIT.2022.3166073

Information Rate Optimization for the Non-Regenerative Linear MIMO Relay Channel with a Direct Link and Variable Duty Cycle♯

Giorgio Taricco, *Fellow, IEEE*

***Abstract*—We consider the optimization of a two-hop linear relay channel based on an amplify-and-forward Multiple-Input Multiple-Output (MIMO) relay. The relay is assumed to derive the output signal by applying a Relay Transform Matrix (RTM) applied to the input signal. Assuming perfect channel state information about the channel at the relay and iid transmitted symbols, the RTM is optimized according to two different criteria: *i)* MIMO information rate; *ii)* information rate based on Orthogonal Space–Time Block Codes. The two assumptions have been addressed in part in the literature. The optimization problem is reduced to a manageable convex form, whose KKT equations are explicitly solved. Then, a parametric solution is given, which yields the power constraint and the information rate achieved with uncorrelated transmitted symbols as functions of a positive indeterminate. The solution for a given average power constraint at the relay is amenable to a *water-filling-like* algorithm, and extends earlier literature results addressing the case without the direct link. The duty cycle of the two-hop relaying process is also addressed in the general form of the achievable rate. Simulation results are reported, which are relevant to a Rayleigh fading MIMO relay channel and the role of the direct link SNR is precisely assessed. Duty cycle optimization is also considered by a numerical example.**

***Index Terms*—MIMO, Relay channels, Information rate, Convex Optimization, Water-filling.**

I. Introduction

Wireless communication systems have been using relaying techniques for several decades in order to extend the range coverage of radio channels. Among the benefits, relays help to combat shadowing and fading effects which may limit the signal propagation in wireless environments. Back in the day, the concept of relaying has been rationalized, from an information theoretical point of view, by the introduction of the three-terminal channel model (source-relay-destination) in the seminal papers by Van Der Meulen [2] and Cover and El Gamal [3], which determined the achievable rate under several operating conditions. During the last two decades, several results emerged in the framework of single and multiple antenna systems. Concerning single-antenna systems, Sendonaris *et al.* studied the effects of relaying as a user cooperation diversity technique to increase the cellular coverage of third-generation systems based on CDMA [4]; Nabar *et al.* investigated different time-division multiple-access-based cooperative protocols with relay terminals operating in either amplify-and-forward or decode-and-forward modes by using the achievable rate as the metric of interest [5]; Laneman *et al.* proposed low-complexity cooperative diversity protocols to combat multipath fading in wireless channels by using several strategies including fixed relaying schemes [Amplify-and-Forward (AF) and Decode-and-Forward (DF)], adaptive relaying schemes, and incremental relaying schemes based upon limited feedback from the destination terminals [6]; Host-Madsen *et al.* provided lower and upper bounds to the outage and ergodic capacity of a three-terminal wireless relay channel in Rayleigh fading while taking into account practical constraints at the relay node and the impact of power allocation [7].

Relaying based on Multiple-Input Multiple-Output (MIMO) wireless terminals has been studied in [8], [9]. Specifically, joint transmission and reception at the relay was addressed in the paper by Wang *et al.* [8] but, as pointed out by Tang and Hua, [9], it may entail unwanted side effects since, typically, the transmitted signal power at the relay overshadows the power of the received signal. As a result, a more practical approach consists of keeping the reception and transmission processes at the relay orthogonal with respect to each other. Orthogonality can be implemented by operating the system in a two-hop time division or by frequency-domain division multiple access scheme.

Focusing on the relayed signal, two basic approaches have been considered in the literature, which can be classified as *regenerative* or *non-regenerative*. The regenerative approach consists of rebuilding the transmitted signal after decoding the received signal, and is commonly referred to as *decode-and-forward* (DF). The non-regenerative consists of forwarding the received signal after amplification, thereby including the received noise. This latter approach is commonly referred to as *amplify-and-forward* (AF). For single-antenna systems, it has been observed that AF schemes are advantageous in terms of achievable diversity order with respect to DF schemes while the situation is not clearly understood for capacity. Nevertheless, AF schemes offer a number of benefits making them preferable to DF schemes [9]. More recently, it has been pointed out that AF schemes enable to retain the soft information of the transmitted signal and guarantee a limited signal delay at the same time [10]–[12].

In the framework of MIMO-AF relay schemes, the transmitted signal is obtained by the joint amplification of the different received signal components so that it can be characterized by a *Relay Transform Matrix* (RTM), which derives the transmitted

♯ Giorgio Taricco (gtaricco@ieee.org) is with Politecnico di Torino (DET). A part of these results have been presented in IEEE ISIT 2021 [1].

signal vector through multiplication by the received signal vector. Following the classification introduced by Tang and Hua [9], we consider three operating schemes for the MIMO relay channel considered: $i)$ Direct Link without Relay; $ii)$ Relay without Direct Link; and $iii)$ Relay with Direct Link. A key contribution from [9] is the derivation of the information-theoretically optimum RTM (i.e., maximizing the information rate corresponding to iid transmitted symbols) for the second operating scheme (Relay without Direct Link). The authors also considered the more general third operating scheme (Relay with Direct Link) but didn't find the optimum RTM in this case and claimed this case to be an open problem [9, p.1400]. This operating scheme was also considered by Shariat and Gazor [10], who focused on the optimization of the "capacity" constrained to the use of Orthogonal Space–Time Block Codes (OSTBC). Their approach is also equivalent to the maximization of the overall Signal-to-Noise Ratio (SNR).

In this work we present an algorithm to derive the RTM optimizing the achievable rate of a two-hop relay channel with iid transmitted symbols. This achievable rate may not be identified with the *capacity* of the relay channel for several reasons, among which the following: $i)$ we do not optimize the input covariance matrix but assume iid transmitted symbols; $ii)$ we constrain the relay channel to transmit a symbol vector obtained linearly from the receive symbol vector (amplify-and-forward operation); and $iii)$ we assume that the number of channel uses is the same for both hops. Please refer to [13]–[15] for additional insight on the subject. We shall refer to the mutual information with iid transmitted symbols as *Symmetric Achievable Rate* (SAR) and to the SAR corresponding to the relay channel under study as *Relay Channel Symmetric Achievable Rate* (RCSAR) in the rest of the paper. Furthermore, if OSTBC is assumed to be used, we shall refer to the corresponding RCSAR as OSTBC-RCSAR.

The above simplifying assumptions have the goal to make the optimization problem solvable and are aligned with the assumptions made in several works from the literature, among which [9], [10].

Nevertheless, the case considered here is more general than [9], [10] for several reasons. First of all, we allow the number of transmit and receive antennas at the relay to be arbitrarily different, as well as the channel matrix ranks. On the contrary, it was assumed in [9] that the number of transmit and receive antennas at the relay was the same and [10] assumed that the rank of the source to destination channel matrix ($\boldsymbol{H}_1$ in this paper) was equal to the number of receive antennas, so that the case $t < r$ (see Fig. 1 for the definitions) was not included. Additionally, the solution presented here applies to the joint direct link and relay transmission case (labeled as "Case (C) Relay With Direct Link" in [9]), recognized as an *open problem* by the authors of [9]. Our solution can be obtained, for a specific relay power constraint, by resorting to a water-filling-like algorithm, bearing some similarity with [9, Sec.IV] (which is nevertheless not applicable to this case). For validation purposes, we report numerical simulation results coherent with those from [9, (B) Relay Without Direct Link] by forcing the direct link channel matrix to zero. Then, we extend the analysis by considering also the case of a complete relay channel, including the direct link, first with an overall constant number of antennas in the relay channel, next, with different number of antennas.

We also consider the impact of the duty cycle on the two-hop relaying process. We present a formula for the achievable rate including the effects of the duty cycle on the achievable rate itself and on the power constraints. We illustrate by numerical examples how is it possible to optimize the duty cycle and maximize the RCSAR.

Summarizing, the paper organization is as follow. Section II introduces the system model for the MIMO relay channel with all relevant parameters which characterize it completely. Then, Section III solves the optimization problems corresponding to the RCSAR and to the OSTBC-RCSAR in the general case of arbitrary channel matrix ranks and dimensions. Section III-A addresses RCSAR optimization with respect to the RTM and extends the work of [9]. Section III-B proposes the relevant parametric solution. Section III-C addresses OSTBC-RCSAR optimization with respect to the RTM and extends the work of [10]. Section III-D proposes the relevant parametric solution. Section IV collects three types of relay channel scenarios to illustrate the application of the theoretical results of the previous section. The first scenario consists of a relay channel without the direct link and is considered for validation and comparison with the results of [9]. The other scenarios consider a complete (with direct link) relay channel with constant number of antennas (where [10] is applicable in the case of OSTBC-RCSAR) an a second scenario with different numbers of antennas (where [10] is not applicable even in the case of OSTBC-RCSAR). One of the previous scenarios is further investigated with variable duty cycle in order to optimize the portion of time-frequency resources to dedicate to direct link transmission and to relaying. Concluding remarks are collected in Section V.

II. System Model

We consider a MIMO linear relay channel consisting of three nodes: the source (S) equipped with t transmit antennas; the destination (D), equipped with r receive antenna; and the relay (R), equipped with u transmit and s receive antennas. The channel matrices corresponding to the three different links of interest are labeled as $\boldsymbol{H}_0$ (S→D), $\boldsymbol{H}_1$ (S→R), and $\boldsymbol{H}_2$ (R→D). The system operates in *two-hop relaying* mode: the source transmits during the first hop and the relay during the second hop.

The average power transmitted by the source and the relay are upper bounded by P_1 and P_2, respectively. We assume that the two hops allocate fractions θ and $\bar{\theta} \triangleq 1-\theta$ of the number of available time-frequency slots, respectively. This implies that the average power bounds, restricted to the respective operating hops, increase to $\frac{P_1}{\theta}$ and $\frac{P_2}{\bar{\theta}}$, respectively.

Since we are considering a regenerative system, where the relay doesn't decode the received signal, relaying consists of transmitting only a fraction $\bar{\theta}/\theta$ of the received symbols. This corresponds to *puncturing* the channel code used by the source and must be implemented by a proper puncturing pattern.

This *variable duty cycle* relaying scheme requires that the inequality $\bar{\theta} \leq \theta$ holds or, equivalently, that $\theta \geq \frac{1}{2}$.

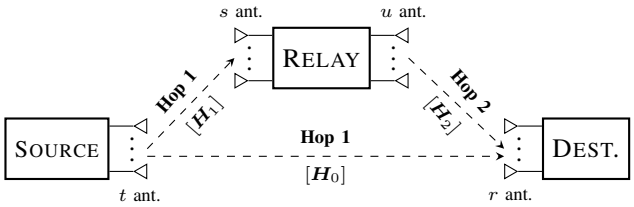

Fig. 1. System block diagram. Transmission occurs in two time/frequency slots (hops) so that the received signal at the destination arrives alternately from the source and from the relay.

The linear relay applies a $u \times s$ *Relay Transformation Matrix* (RTM) $\boldsymbol{X}$ to the received signal before forwarding it to the destination in the second hop. The resulting channel equations are given as follows:

$$\boldsymbol{y}_0 = \boldsymbol{H}_0\boldsymbol{x} + \boldsymbol{z}_0 \quad \text{(Hop 1, S}\rightarrow\text{D)} \quad (1)$$

$$\boldsymbol{y}_1 = \boldsymbol{H}_1\boldsymbol{x} + \boldsymbol{z}_1 \quad \text{(Hop 1, S}\rightarrow\text{R)} \quad (2)$$

$$\begin{aligned}\boldsymbol{y}_2 &= \boldsymbol{H}_2\boldsymbol{X}\boldsymbol{y}_1 + \boldsymbol{z}_2 \quad \text{(Hop 2, R}\rightarrow\text{D)} \quad (3)\\ &= \boldsymbol{H}_2\boldsymbol{X}\boldsymbol{H}_1\boldsymbol{x} + \boldsymbol{H}_2\boldsymbol{X}\boldsymbol{z}_1 + \boldsymbol{z}_2\end{aligned}$$

We assume, w.l.o.g., that the received noise components are iid $\mathcal{CN}(0,1)$[1] (optionally, we could pre-multiply the received vectors and the channel matrices by the inverse matrix square roots of the corresponding noise correlation matrices). Then,

$$\boldsymbol{z}_0, \boldsymbol{z}_2 \sim \mathcal{CN}(\boldsymbol{0}, \boldsymbol{I}_r), \quad \boldsymbol{z}_1 \sim \mathcal{CN}(\boldsymbol{0}, \boldsymbol{I}_s) \quad (4)$$

The equivalent channel equation becomes

$$\boldsymbol{y} = \begin{pmatrix}\boldsymbol{H}_0\\ \boldsymbol{H}_2\boldsymbol{X}\boldsymbol{H}_1\end{pmatrix}\boldsymbol{x} + \begin{pmatrix}\boldsymbol{z}_0\\ \boldsymbol{H}_2\boldsymbol{X}\boldsymbol{z}_1 + \boldsymbol{z}_2\end{pmatrix} \quad (5)$$

After decorrelating the second hop noise component, it can be written as follows:

$$\tilde{\boldsymbol{y}} = \begin{pmatrix}\boldsymbol{H}_0\\ (\boldsymbol{H}_2\boldsymbol{X}\boldsymbol{X}^{\mathsf{H}}\boldsymbol{H}_2^{\mathsf{H}} + \boldsymbol{I}_r)^{-1/2}\boldsymbol{H}_2\boldsymbol{X}\boldsymbol{H}_1\end{pmatrix}\boldsymbol{x} + \tilde{\boldsymbol{z}} \quad (6)$$

where $\tilde{\boldsymbol{z}} \sim \mathcal{CN}(\boldsymbol{0}, \boldsymbol{I}_{2r})$. This channel equation and the assumption of iid transmitted symbols lead to the expression of the relay channel mutual information reported in the following eq. (7), referred to hereafter as Relay Channel Symmetric Achievable Rate (RCSAR).

Remark II.1 Throughout the paper, the source is assumed to have no knowledge about the Channel State Information (CSI), represented by the channel matrices $\boldsymbol{H}_0, \boldsymbol{H}_1, \boldsymbol{H}_2$. On the contrary, the relay has perfect knowledge of the CSI, and the destination knows exactly the channel matrices $\boldsymbol{H}_0$ and $\boldsymbol{H}_2$.

This can be implemented as follows: $i)$ the relay estimates $\boldsymbol{H}_1$ by using known pilot symbols sent by the source; $ii)$ the destination estimates $\boldsymbol{H}_0$ and $\boldsymbol{H}_2$ by using known pilot symbols sent by the source and the relay, respectively; and $iii)$ the estimates of $\boldsymbol{H}_0$ and $\boldsymbol{H}_2$ are fed back to the relay through a control channel.

[1]We use the notation $\boldsymbol{z} \sim \mathcal{CN}(\boldsymbol{\mu}, \boldsymbol{\Sigma})$ to represent the circularly-symmetric complex Gaussian distribution of a random vector $\boldsymbol{z}$. The corresponding pdf is defined by $f_{\boldsymbol{z}}(\boldsymbol{z}) = \det(\pi\boldsymbol{\Sigma})^{-1}\exp[-(\boldsymbol{z}-\boldsymbol{\mu})^{\mathsf{H}}\boldsymbol{\Sigma}^{-1}(\boldsymbol{z}-\boldsymbol{\mu})]$.

The perfect CSI assumption at the relay and the destination (the latter limited to $\boldsymbol{H}_0$ and $\boldsymbol{H}_2$) can be approximated closely by allocating a sufficient amount of time-frequency resources to the pilot symbol transmission and to the feedback channel.

III. RTM Optimization

In this section we address the calculation of the optimum RTM based on the assumption that the relay *knows* all the channel matrices involved in eqs. (1)-(3). Specifically, we look for the RTM which maximizes the two-hop RCSAR.

A. Optimum RTM

We follow the method illustrated in [16] to calculate the relay channel mutual information with some variations due to the fact that our relay is not regenerative. In the case considered, we don't need using the lower and upper bounds reported in [16] because the mutual information stems from channel equation (6). The equivalent channel $\boldsymbol{x} \rightarrow \tilde{\boldsymbol{y}}$ is a standard MIMO Gaussian channel whose capacity is achieved by Gaussian inputs. In the absence of CSI at the transmitting source, we assume that the transmitted vector is $\mathcal{CN}(\boldsymbol{0}, p\boldsymbol{I}_t)$, i.e., the input covariance matrix is given by $\boldsymbol{Q}_x = p\boldsymbol{I}_t$ for some $p > 0$ deriving from the power constraints. Then, after some algebra, we obtain the following expression of the RCSAR:

$$\begin{aligned}\mathcal{I}(\theta) = \bar{\theta}\log_2\det\Big\{&\boldsymbol{I}_t + \frac{P_1}{\theta t}\Big[\boldsymbol{H}_0^{\mathsf{H}}\boldsymbol{H}_0 + \boldsymbol{H}_1^{\mathsf{H}}\boldsymbol{X}^{\mathsf{H}}\boldsymbol{H}_2^{\mathsf{H}}\\ &(\boldsymbol{I}_r + \boldsymbol{H}_2\boldsymbol{X}\boldsymbol{X}^{\mathsf{H}}\boldsymbol{H}_2^{\mathsf{H}})^{-1}\boldsymbol{H}_2\boldsymbol{X}\boldsymbol{H}_1\Big]\Big\}\\ &+ (\theta - \bar{\theta})\log_2\det\Big\{\boldsymbol{I}_t + \frac{P_1}{\theta t}\boldsymbol{H}_0^{\mathsf{H}}\boldsymbol{H}_0\Big\}\end{aligned} \quad (7)$$

The expression is justified by the fact that for a fraction $\bar{\theta}$ of the available time-frequency resources, the relay channel is modeled by eq. (6), where both the direct link and the relay link are used, and for the remaining fraction $(\theta - \bar{\theta})$ of the available time-frequency resources, the relay channel has only the direct link available. Moreover, the duty cycle θ affects the average transmitted power, which is increased by the factor $\frac{1}{\theta}$. The average power constraint at the relay becomes:

$$\operatorname{tr}\Big\{\boldsymbol{X}\Big(\boldsymbol{I}_s + \frac{P_1}{\theta t}\boldsymbol{H}_1\boldsymbol{H}_1^{\mathsf{H}}\Big)\boldsymbol{X}^{\mathsf{H}}\Big\} \leq \frac{P_2}{\bar{\theta}}. \quad (8)$$

The optimum RTM (maximizing the RCSAR from (7) under the constraint (8)) is given by the following Theorem.

Theorem 1 *Given the two-hop MIMO relay channel described by eqs.* (1)-(3) *with average source and relay power constraints P_1 and P_2, the optimum (maximizing the SAR) RTM $\boldsymbol{X}$ is given by*

$$\boldsymbol{X} = \widetilde{\boldsymbol{U}}_B\widetilde{\boldsymbol{\Lambda}}_B^{-1/2}\widetilde{\boldsymbol{\Lambda}}^{1/2}\widetilde{\boldsymbol{U}}_A^{\mathsf{H}}, \quad (9)$$

where the matrices $\widetilde{\boldsymbol{U}}_B, \widetilde{\boldsymbol{\Lambda}}_B, \widetilde{\boldsymbol{U}}_A$ are obtained by the "thin" unitary diagonalizations (UD's) [17, Th. 7.3.2]:[2]

$$\boldsymbol{A} = \widetilde{\boldsymbol{U}}_A\widetilde{\boldsymbol{\Lambda}}_A\widetilde{\boldsymbol{U}}_A^{\mathsf{H}}, \qquad \boldsymbol{B} = \widetilde{\boldsymbol{U}}_B\widetilde{\boldsymbol{\Lambda}}_B\widetilde{\boldsymbol{U}}_B^{\mathsf{H}}. \quad (10)$$

[2]A "thin" UD $\boldsymbol{U}\boldsymbol{\Lambda}\boldsymbol{U}^{\mathsf{H}}$ of an $n \times n$ matrix is characterized by an $m \times m$ diagonal matrix $\boldsymbol{\Lambda}$ whose diagonal entries are sorted in nonincreasing order, i.e., $(\boldsymbol{\Lambda})_{i,i} \geq (\boldsymbol{\Lambda})_{i+1,i+1}$ for $i = 1, \ldots, m-1$ and a semi-unitary $n \times m$ matrix $\boldsymbol{U}$ with the property that $\boldsymbol{U}^{\mathsf{H}}\boldsymbol{U} = \boldsymbol{I}_m$.

where

$$\boldsymbol{A} \triangleq \boldsymbol{H}_1\left(\frac{\theta t}{P_1}\boldsymbol{I}_t + \boldsymbol{H}_0^{\mathsf{H}}\boldsymbol{H}_0 + \boldsymbol{H}_1^{\mathsf{H}}\boldsymbol{H}_1\right)^{-1}\boldsymbol{H}_1^{\mathsf{H}} \quad (11)$$

$$\boldsymbol{B} \triangleq \boldsymbol{H}_2^{\mathsf{H}}\boldsymbol{H}_2, \qquad \boldsymbol{C} \triangleq \boldsymbol{I}_s + \frac{P_1}{\theta t}\boldsymbol{H}_1\boldsymbol{H}_1^{\mathsf{H}} \quad (12)$$

We also have

$$\widetilde{\boldsymbol{\Lambda}} \triangleq \mathrm{diag}(x_1, \ldots, x_\rho, \underbrace{0, \ldots, 0}_{\rho_B - \rho}) \quad (13)$$

where $\rho \triangleq \min(s, \rho_B)$ *and* $\rho_B \triangleq \mathrm{rank}(\boldsymbol{B}) = \mathrm{rank}(\boldsymbol{H}_2) \leq \min(u, r)$. *The diagonal matrix* $\widetilde{\boldsymbol{\Lambda}}_A$ *is possibly extended by zero padding to the size* $\rho_B \times \rho_B$. *The matrix* $\widetilde{\boldsymbol{\Lambda}}$ *has* $\rho \leq \rho_B$ *possibly positive eigenvalues, obtained by solving the convex optimization problem*

$$\begin{cases} \min\limits_{\boldsymbol{x}\geq\boldsymbol{0}} & -\sum\limits_{i=1}^{\rho} \ln\left\{1 - \dfrac{\alpha_i}{1+x_i}\right\} \\ \text{s.t.} & \sum\limits_{i=1}^{\rho} \beta_i x_i \leq \dfrac{P_2}{\bar{\theta}}, \quad x_i \geq 0, i = 1, \ldots, \rho \end{cases} \quad (14)$$

where, for $i = 1, \ldots, \rho$,

$$\alpha_i \triangleq (\widetilde{\boldsymbol{\Lambda}}_A)_{i,i}, \qquad \beta_i \triangleq \frac{(\widetilde{\boldsymbol{U}}_A^{\mathsf{H}}\boldsymbol{C}\widetilde{\boldsymbol{U}}_A)_{i,i}}{(\widetilde{\boldsymbol{\Lambda}}_B)_{i,i}} \quad (15)$$

Proof: See App. A. ■

B. Parametric Water-Filling solution

We can get a closed-form parametric solution of the optimization problem (14) in Theorem 1 based on a single positive parameter ξ.[3] To this end, we define[4]

$$\varphi_i(\xi) \triangleq \left\{\frac{\alpha_i}{2} - 1 + \sqrt{\frac{\alpha_i^2}{4} + \frac{\alpha_i}{\beta_i}\xi}\right\}_+, \; i = 1, \ldots, \rho. \quad (16)$$

These functions provide the components of the vector $\boldsymbol{x}$, solution of the optimization problem (14) in Theorem 1, as $x_i = \varphi_i(\xi)$. Accordingly, we obtain two parametric equations:

$$\frac{P_2}{\bar{\theta}} = \sum_{i=1}^{\rho} \beta_i \varphi_i(\xi) \quad (17)$$

$$\mathcal{I}(\theta) = \theta \log_2 \det\left\{\boldsymbol{I}_t + \frac{P_1}{\theta t}(\boldsymbol{H}_0^{\mathsf{H}}\boldsymbol{H}_0 + \boldsymbol{H}_1^{\mathsf{H}}\boldsymbol{H}_1)\right\} + \theta \sum_{i=1}^{\rho} \log_2\left\{1 - \frac{\alpha_i}{1+\varphi_i(\xi)}\right\} \quad (18)$$

These expressions are obtained by solving the KKT equations corresponding to the optimization problem (14) and are derived in detail in App. B.

The uniqueness of the solution of (17) stems from the fact that the functions $\varphi_i(\xi)$ are monotonically increasing for $\xi > \xi_i \triangleq (1-\alpha_i)\beta_i$. Since $\varphi_i(\xi) = 0$ for $\xi \leq \xi_i$, we can find solve (17) numerically by dividing the real positive line $\{\xi : \xi > 0\}$ through the sorted thresholds ξ_i and considering over each interval so determined only the positive functions. This remains nevertheless a nonlinear equation. The approach recalls the solution of the water-filling equation arising in the case of independent additive Gaussian channels with an overall average power constraint [18].

[3] The variable ξ is a dummy parameter corresponding to the inverse of a Lagrange multiplier (λ_0) defined in Appendix B. It turns out that the fact that the power constraint must be satisfied with equality (as shown at the end of Appendix A) implies that $\lambda_0 > 0$ and hence ξ is finite and positive.

[4] Hereafter, $\{\cdot\}_+ \triangleq \max(0, \cdot)$.

C. RTM optimization based on OSTBC-RCSAR

In this section we consider the case of Orthogonal Space–Time Block Coding (OSTBC) at the transmitter and maximize the corresponding RCSAR with respect to the RTM. The OSTBC mutual information has been characterized in [19]. This approach has been followed in [10] where the authors also assumed that the matrix $\boldsymbol{H}_1\boldsymbol{H}_1^{\mathsf{H}}$ has full rank s. This assumption is not satisfied, for example, when $t < s$, and limits the generality of that result. For this reason, we derive the optimum RTM in the general case.

The OSTBC-RCSAR with symbol rate $R \leq 1$ of the MIMO relay channel is given by [19]:

$$\mathcal{I}_{\mathsf{OSTBC}}(\theta) = \bar{\theta} R \log_2\left\{1 + \frac{P_1}{\theta t R}\,\mathrm{tr}\left[\boldsymbol{H}_0^{\mathsf{H}}\boldsymbol{H}_0 + \boldsymbol{H}_1^{\mathsf{H}}\boldsymbol{X}^{\mathsf{H}}\boldsymbol{H}_2^{\mathsf{H}} (\boldsymbol{I}_r + \boldsymbol{H}_2\boldsymbol{X}\boldsymbol{X}^{\mathsf{H}}\boldsymbol{H}_2^{\mathsf{H}})^{-1}\boldsymbol{H}_2\boldsymbol{X}\boldsymbol{H}_1\right]\right\} + (\theta - \bar{\theta}) R \log_2\left\{1 + \frac{P_1}{\theta t R}\,\mathrm{tr}(\boldsymbol{H}_0^{\mathsf{H}}\boldsymbol{H}_0)\right\} \quad (19)$$

The optimum RTM (maximizing the above RCSAR over $0 \leq R \leq 1$, and therefore corresponding to $R = 1$) is given in the following Theorem.

Theorem 2 *Given the two-hop MIMO relay channel described by* (1)-(3) *with average source and relay power constraints* P_1 *and* P_2, *the optimum (OSTBC-RCSAR-maximizing) RTM* $\boldsymbol{X}$ *is given by*

$$\boldsymbol{X} = \widetilde{\boldsymbol{U}}_B\widetilde{\boldsymbol{\Lambda}}_B^{-1/2}\widetilde{\boldsymbol{\Lambda}}^{1/2}\widetilde{\boldsymbol{U}}_A^{\mathsf{H}}, \quad (20)$$

where the matrices $\widetilde{\boldsymbol{U}}_B, \widetilde{\boldsymbol{\Lambda}}_B, \widetilde{\boldsymbol{U}}_A$ *are obtained by the "thin" UD's*

$$\check{\boldsymbol{A}} = \widetilde{\boldsymbol{U}}_A\widetilde{\boldsymbol{\Lambda}}_A\widetilde{\boldsymbol{U}}_A^{\mathsf{H}}, \qquad \check{\boldsymbol{B}} = \widetilde{\boldsymbol{U}}_B\widetilde{\boldsymbol{\Lambda}}_B\widetilde{\boldsymbol{U}}_B^{\mathsf{H}}. \quad (21)$$

where

$$\check{\boldsymbol{A}} \triangleq \boldsymbol{H}_1\boldsymbol{H}_1^{\mathsf{H}}, \quad \check{\boldsymbol{B}} \triangleq \boldsymbol{H}_2^{\mathsf{H}}\boldsymbol{H}_2, \quad \boldsymbol{C} \triangleq \boldsymbol{I}_s + \frac{P_1}{\theta t}\boldsymbol{H}_1\boldsymbol{H}_1^{\mathsf{H}} \quad (22)$$

We define $\widetilde{\boldsymbol{\Lambda}}$ *as in* (13), $\rho \triangleq \min(s, \rho_B)$ *and* $\rho_B \triangleq \mathrm{rank}(\boldsymbol{B}) = \mathrm{rank}(\boldsymbol{H}_2) \leq \min(u, r)$. $\widetilde{\boldsymbol{\Lambda}}_A$ *is possibly extended by zero padding to the size* $\rho_B \times \rho_B$. *The* $x_i, i = 1, \ldots, \rho$ *are obtained by solving the optimization problem*

$$\begin{cases} \min\limits_{\boldsymbol{x}\geq\boldsymbol{0}} & \sum\limits_{i=1}^{\rho} \dfrac{\alpha_i}{1+x_i} \\ \text{s.t.} & \sum\limits_{i=1}^{\rho} \beta_i x_i \leq \dfrac{P_2}{\bar{\theta}}, \quad x_i \geq 0, i = 1, \ldots, \rho \end{cases} \quad (23)$$

where, for $i = 1, \ldots, \rho$,

$$\alpha_i \triangleq (\widetilde{\boldsymbol{\Lambda}}_A)_{i,i}, \qquad \beta_i \triangleq \frac{(\widetilde{\boldsymbol{U}}_A^{\mathsf{H}}\boldsymbol{C}\widetilde{\boldsymbol{U}}_A)_{i,i}}{(\widetilde{\boldsymbol{\Lambda}}_B)_{i,i}} \quad (24)$$

Proof: See App. C. ■

Remark III.1 As illustrated in detail in [19], the OSTBC-RCSAR (19) and the RCSAR (7) are linked by a simple relationship. Denoting the eigenvalues of the matrix

$$\frac{1}{t}\Big[\boldsymbol{H}_0^{\mathsf{H}}\boldsymbol{H}_0+\boldsymbol{H}_1^{\mathsf{H}}\boldsymbol{X}^{\mathsf{H}}\boldsymbol{H}_2^{\mathsf{H}}(\boldsymbol{I}_r+\boldsymbol{H}_2\boldsymbol{X}\boldsymbol{X}^{\mathsf{H}}\boldsymbol{H}_2^{\mathsf{H}})^{-1}\boldsymbol{H}_2\boldsymbol{X}\boldsymbol{H}_1\Big] \tag{25}$$

as ζ_i, we have

$$\mathcal{I}(\theta)=\theta\sum_{i=1}^{t}\log_2\left(1+\frac{P_1}{\theta}\zeta_i\right) \tag{26}$$

$$\mathcal{I}_{\mathsf{OSTBC}}(\theta)=\theta\log_2\left(1+\frac{P_1}{\theta}\sum_{i=1}^{t}\zeta_i\right). \tag{27}$$

The simple inequality

$$1+\frac{P_1}{\theta}\sum_{i=1}^{t}\zeta_i\leq\prod_{i=1}^{t}\left(1+\frac{P_1}{\theta}\zeta_i\right) \tag{28}$$

implies that the OSTBC-RCSAR is always upper bounded by the RCSAR and the two values tend to coincide as $P_1\downarrow 0$. One can argue that this is a consequence of the OSTBC structure which limits the range of possible input covariance matrix whose full extent is considered to derive the RCSAR. This relationship carries on to the parametric expressions of the optimum capacities reported in eqs. (18) and (31), corresponding to the MIMO and OSTBC cases, respectively.

D. Parametric Water-Filling solution

Here we provide a closed-form parametric solution to the optimization problem considered in Theorem 2, based on an independent positive variable ξ (cfr. Footnote 3). Using the definitions of Theorem 2, we define

$$\psi_i(\xi)\triangleq\left\{\xi\sqrt{\frac{\alpha_i}{\beta_i}}-1\right\}_+ \tag{29}$$

Accordingly, we obtain these two parametric equations:

$$\frac{P_2}{\bar{\theta}}=\sum_{i=1}^{\rho}\beta_i\psi_i(\xi) \tag{30}$$

$$\mathcal{I}(\theta)=\theta\log_2\left\{1+\frac{P_1}{\theta t}\left(\boldsymbol{H}_0^{\mathsf{H}}\boldsymbol{H}_0+\boldsymbol{H}_1^{\mathsf{H}}\boldsymbol{H}_1-\sum_{i=1}^{\rho_A}\frac{(\boldsymbol{\Lambda}_A)_{i,i}}{1+\psi_i(\xi)}\right)\right\} \tag{31}$$

These expressions are derived in detail in App. D.

IV. Numerical results

The numerical results in this section are presented to validate the algorithms derived in cases already handled in the literature and to show their applicability to cases where the literature algorithms are not applicable.

A. Validation of the results

Here, we validate our results against [9, Figs. 3 and 4], where the number of antennas is $t=r=u=s=M=4$, and the ergodic[5] RCSAR corresponding to iid Rayleigh channel matrices and no direct link is considered (more precisely, the entries of $\boldsymbol{H}_1,\boldsymbol{H}_2$ are iid $\mathcal{CN}(0,1)$ and $\boldsymbol{H}_0\equiv\boldsymbol{0}$). The SNR's are defined as:

$$\rho_1\triangleq\frac{P_1}{M},\quad\rho_2\triangleq\frac{P_2}{M}. \tag{32}$$

We also use the same normalization conditions of [9], namely: $i)$ fixed duty cycle $\theta=\frac{1}{2}$; $ii)$ duty cycle not accounted for in the ergodic RCSAR (which corresponds to multiply the rhs of eq. (7) by 2); $iii)$ duty cycle not accounted for in the average powers (which corresponds to replacing $\frac{P_1}{\theta}$ by P_1 and $\frac{P_2}{\bar{\theta}}$ by P_2 in (7) and (8)).

Fig. 2 illustrates the ergodic RCSAR vs. ρ_1 at $\rho_2=10$ dB while Fig. 3 illustrates the ergodic RCSAR vs. ρ_2 at $\rho_1=10$ dB. Each figure reports six curves with a composite label consisting of two tags: the first one denotes the type of RTM used (OPT1, OPT2, NAF); and the second one denotes the type of RCSAR plotted. The types of RTM's considered are: $i)$ OPT1: RTM maximizing the RCSAR (7); $ii)$ OPT2: RTM maximizing the OSTBC-RCSAR (19); $iii)$ NAF: Naive Amplify and Forward, where the RTM is a scaled identity matrix.

Notice that we have introduced mismatches between the RTM optimization and the type of RCSAR reported. For example, the curve OPT1-OSTBC reports the OSTBC-RCSAR obtained by using an RTM optimized for the RCSAR, and the curve OPT2-CAP reports the RCSAR obtained by using an RTM optimized for the OSTBC-RCSAR.

The goal of this is to outline the effects of using the simpler RTM optimization, known from the literature [10] and based on the adoption of the OSTBC-RCSAR as objective function, to maximize the actual RCSAR given in (7).

The results labeled by OPT1-CAP and NAF-CAP agree with [9, Figs. 3 and 4]. They also meet our intuitive expectations. The OPT1 RTM maximizes the ergodic RCSAR and is suboptimal for the OSTBC-RCSAR. The OPT2 RTM maximizes the ergodic OSTBC-RCSAR and is suboptimal for the ergodic RCSAR. The NAF RTM exhibits the expected performance degradation (except in the case OPT2-CAP from Fig. 2 where OPT2-CAP is worse than NAF-CAP above a certain ρ_1).

It is noticeable, from Fig. 2, that the OPT2 ergodic RCSAR performance presents a *strong degradation* at large ρ_1, as a consequence of the mismatch between the RCSAR and the OSTBC-RCSAR.

Focusing on the asymptotic behavior of the RCSAR curves in Figs. 2 and 3, we notice a key difference. In Fig. 2, when $\rho_1\to\infty$, all curves converge to different limits, which depend on the fixed value of ρ_2. On the contrary, in Fig. 3, when $\rho_2\to\infty$, all the RCSAR and OSTBC-RCSAR curves converge to the same limits, respectively, which depend

[5] In this work, consistently with the literature, we use the word *ergodic* to refer to the average value with respect to the random realization of the channel matrices.

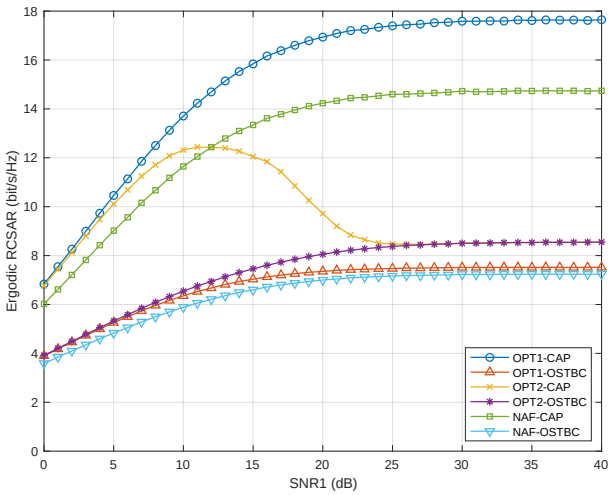

Fig. 2. Plot of the ergodic RCSAR vs. ρ_1 (denoted by SNR1) with $\rho_2 = 10$ dB, iid Rayleigh fading and three types of RTM. $i)$ OPT1: optimum RTM for RCSAR. $ii)$ OPT2: optimum RTM for full-rate OSTBC-RCSAR. $iii)$ NAF: Naive Amplify and Forward, the RTM is a scaled identity matrix.

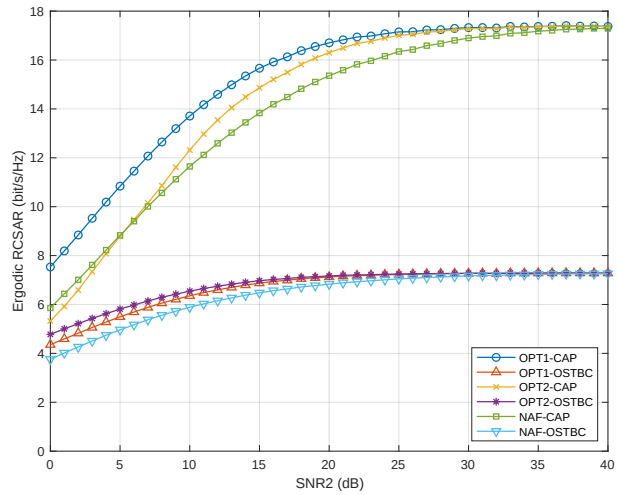

Fig. 3. Plot of the ergodic RCSAR vs. ρ_2 (denoted by SNR2) with $\rho_1 = 10$ dB, iid Rayleigh fading and three types of RTM. $i)$ OPT1: optimum RTM for RCSAR. $ii)$ OPT2: optimum RTM for full-rate OSTBC-RCSAR. $iii)$ NAF: Naive Amplify and Forward, the RTM is a scaled identity matrix.

on the fixed value of ρ_1. The difference is consistent with the following information theoretical interpretation. The relay channel is the cascade of two channels, channel 1 (source to relay) and channel 2 (relay to destination). As such, the data-processing inequality [18] must be satisfied and the overall RCSAR is upper bounded by the RCSAR of each channel. In the case illustrated in Fig. 2, when $\rho_1 \to \infty$, channel 1's SAR goes to infinity so that the RCSAR coincides with that of channel 2, and depends on the RTM. Hence, the different limits. Focusing on OSTBC-RCSAR maximization, when $\rho_1 \to \infty$, we can see that the RTM rank tends to 1, so that the RCSAR and the OSTBC-RCSAR tend to the same limit.

On the contrary, in the case illustrated in Fig. 3, when $\rho_2 \to \infty$, channel 2's SAR goes to infinity so that the RCSAR coincides with channel 1's SAR, which is independent of the RTM. Hence, the coincidence of the limits. Moreover, the upper ergodic RCSAR limits in both figures coincide.

Finally, we notice that the ergodic OSTBC-RCSAR always entails a major loss (even in the full-rate case) with respect to the ergodic RCSAR.

B. Complete Relay Channel — Equal Number of Antennas

Here, we consider a relay channel with direct link, contrary to the scenario considered in Section IV-A. We still assume that all antenna arrays have the same number of antennas, $t = r = u = s = M = 4$, and the channel matrices are iid Rayleigh as before (i.e., all entries of $\boldsymbol{H}_i$ are iid $\mathcal{CN}(0, \eta_i)$ distributed, $i = 0, 1, 2$). Finally, we define the SNR's as

$$\rho_0 \triangleq \eta_0 \frac{P_1}{M}, \quad \rho_1 \triangleq \eta_1 \frac{P_1}{M}, \quad \rho_2 \triangleq \eta_2 \frac{P_2}{M}. \tag{33}$$

Again, we use the normalization of [9] in order to compare the results, namely: $i)$ fixed duty cycle $\theta = \frac{1}{2}$; $ii)$ ergodic RCSAR (7) multiplied by 2; $iii)$ duty cycle not accounted for in the average powers.

Fig. 4 shows the ergodic RCSAR vs. ρ_2 with $\rho_0 = -10$ dB and 10 dB, and $\rho_1 = 10$ dB. Again, the optimum for RCSAR (OPT1), for OSTBC-RCSAR (OPT2) and naive amplify and forward (NAF) RTM's are considered. We notice that, for the low ρ_0, i.e., $\rho_0 = -10$ dB, the results are close to those reported in Fig. 3. This condition is similar to having no direct link because most power passes through the relay. Increasing ρ_0 has a major impact on the performance results, as illustrated. These results allow to assess the trade-offs implied by the presence of the direct link, which is a key contribution of this work.

In a similar way, Fig. 5 plots the ergodic RCSAR vs. ρ_0 with fixed $\rho_1 = 10$ dB and $\rho_2 = 10$ or 20 dB. In this case, the curves increase monotonically with respect to the direct link SNR ρ_0 and saturate to an asymptotic limit as $\rho_2 \to \infty$. By these results we can discern whether the RTM optimization is worthy or the naive amplify and forward is sufficiently good for a given scenario. For example, we can see from Fig. 5 a clear advantage when $\rho_2 = 10$ dB, which decreases progressively by increasing ρ_2. Then, if the relay-to-destination SNR ρ_2 is large (*e.g.,* 20 dB), there is little gain available from RTM optimization, while the gain is substantial when $\rho_2 = 10$ dB.

C. Complete Relay Channel — Different Number of Antennas

In this section, we consider the case of variable number of antennas at the relay. The literature results [9], [10] are not applicable in this case. Again, we assume that the channel matrices are iid Rayleigh (i.e., all entries of $\boldsymbol{H}_i$ are iid $\mathcal{CN}(0, \eta_i)$ distributed, $i = 0, 1, 2$), and the duty cycle is $\theta = \frac{1}{2}$. Contrary to Sections IV-A and IV-B, the proper normalizations from (7) and (8) are used.

We consider a scenario where $t = r = 2$ and $s = u = 2, 4$, or 8, and the SNR's are defined as

$$\rho_0 \triangleq \eta_0 \frac{P_1}{t}, \quad \rho_1 \triangleq \eta_1 \frac{P_1}{t}, \quad \rho_2 \triangleq \eta_2 \frac{P_2}{u}. \tag{34}$$

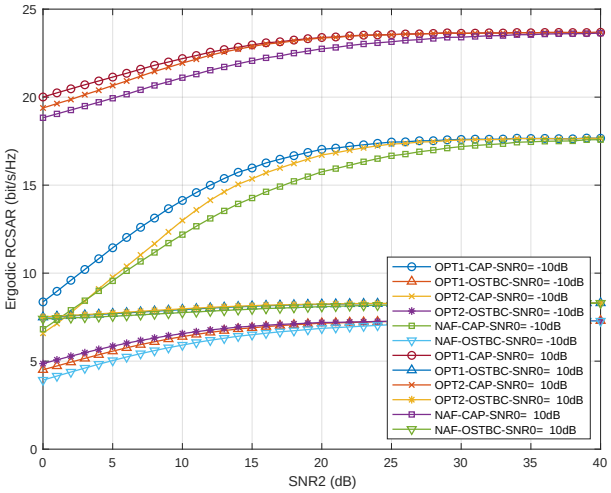

Fig. 4. Plot of the ergodic RCSAR vs. ρ_2 (denoted SNR2) with $\rho_0 = -10, 10$ dB, $\rho_1 = 10$ dB, iid Rayleigh fading and three types of RTM. $i)$ OPT1: optimum RTM for RCSAR. $ii)$ OPT2: optimum RTM for full-rate OSTBC-RCSAR. $iii)$ NAF: Naive Amplify and Forward, the RTM is a scaled identity matrix.

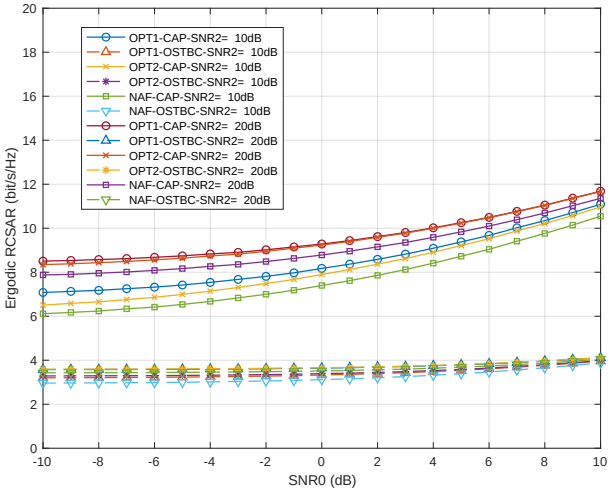

Fig. 5. Plot of the ergodic RCSAR vs. ρ_0 (denoted SNR0) with $\rho_2 = 10, 20$ dB, $\rho_1 = 10$ dB, iid Rayleigh fading and three types of RTM. $i)$ OPT1: optimum RTM for RCSAR. $ii)$ OPT2: optimum RTM for full-rate OSTBC-RCSAR. $iii)$ NAF: Naive Amplify and Forward, the RTM is a scaled identity matrix.

Figs. 6 to 8 show the ergodic RCSAR of this relay channel vs. ρ_2 with $\rho_1 = 10$ dB and two values of $\rho_0 = -10, 10$ dB. We can see that increasing the number of relay antennas is quite beneficial to the relay channel. In fact, the limit ergodic RCSAR with $\rho_0 = \rho_1 = 10$ dB and $\rho_2 \to \infty$ increases from 9.9 to 11.4 and 13.0 bit/s/Hz as the number of relay antennas increases from $s = u = 2$ to 4 and 8, respectively, while the number of transmit and receive antennas at the source and destination remain fixed and equal to 2. Comparatively, the SAR of the direct link without the relay for $\rho_0 = 10$ dB is 7.14 bit/s/Hz [20]. These results show the effectiveness of a MIMO relay with different numbers of antennas on the SAR.

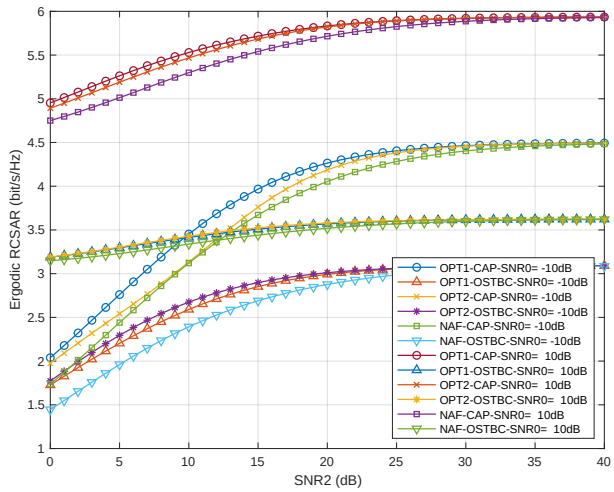

Fig. 6. Plot of the ergodic RCSAR vs. ρ_2 (denoted SNR2) with $\rho_0 = -10, 10$ dB, $\rho_1 = 10$ dB, iid Rayleigh fading, relay channel with $t = r = 2$ and $s = u = 2$, and three types of RTM. $i)$ OPT1: optimum RTM for RCSAR. $ii)$ OPT2: optimum RTM for full-rate OSTBC-RCSAR. $iii)$ NAF: Naive Amplify and Forward, the RTM is a scaled identity matrix.

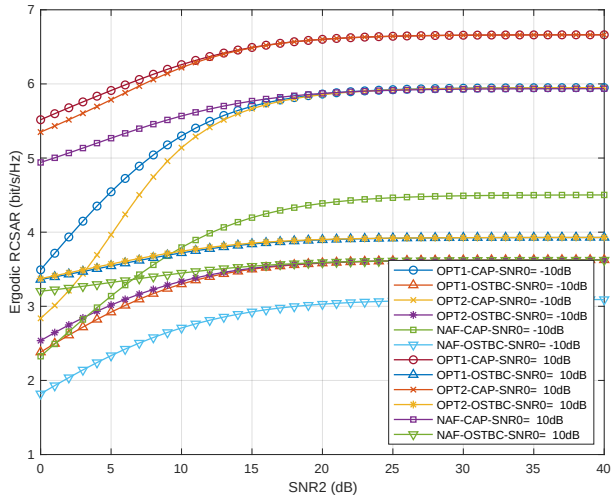

Fig. 7. Same as Fig. 6 but $s = u = 4$.

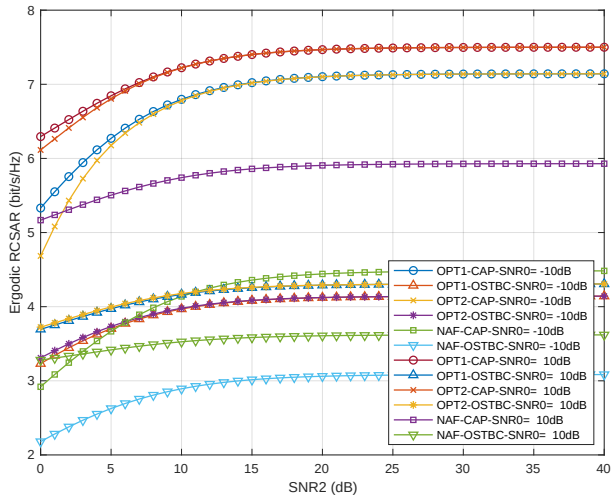

Fig. 8. Same as Fig. 6 but $s = u = 8$.

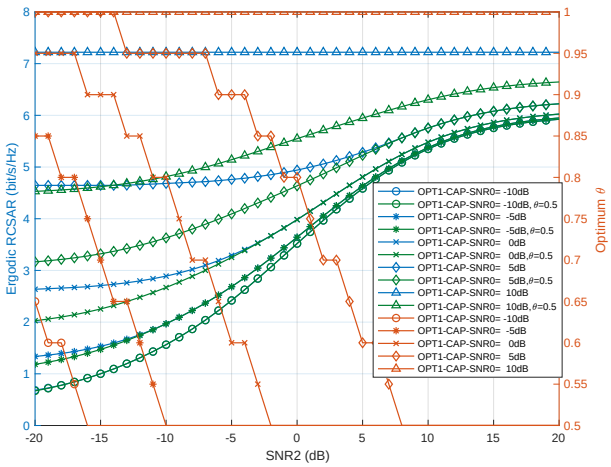

Fig. 9. Same as Fig. 7 but with duty cycle optimization.

D. Duty cycle optimization

In this section we analyze the impact of the duty cycle θ and assume $\theta \in [0.5, 1]$ as explained in Section II. Specifically, we consider one of the numerical examples provided in Section IV-C and study the effect of varying the duty-cycle.

Fig. 9 reports results compatible with those illustrated in Section IV-C in Fig. 7 relevant to the iid Rayleigh scenario with $t = r = 2$ and $s = u = 4$. Only the case OPT1-CAP is reported here, corresponding to the ergodic RCSAR with optimized RTM. Here, we also optimize over the duty cycle $\theta \in [0.5, 1]$. The results corresponding to $\theta = \frac{1}{2}$ are also included.

First of all, we can see that the results for $\theta = \frac{1}{2}$ and $\rho_0 = -10$ and 10 dB coincide with the corresponding results of Fig. 7.

More interestingly, we can see the advantages of optimizing the duty cycle. The diagram reports, quoted on the right-hand vertical axis, the optimum duty cycle θ corresponding to the different values of ρ_0 and ρ_2 (labeled as SNR0 and SNR2, respectively, in the figure).

We can see that, as ρ_2 (the relay to destination SNR) decreases, it becomes more convenient increasing the duty cycle θ, which corresponds to reducing the use of the relay to destination link.

For low direct link SNR ρ_0, the advantage of duty cycle optimization is limited but, as ρ_0 increases, the advantage increases as well, especially for lower values of ρ_2.

The optimum duty cycle curves represent a bridge between two extreme situations: $i)$ the case when using the relay is not convenient since the relay to destination SNR is too low; and $ii)$ the case when the relay to destination SNR is sufficiently high to use the maximum available time-frequency resource share for relaying, which corresponds to a duty cycle $\theta = \frac{1}{2}$, the minimum value.

Summarizing, by duty cycle optimization, one can see if using the relay is convenient or not and, in some cases, if it is possible to optimize the fraction of time-frequency resources to be dedicated to relaying.

V. Conclusions

This work focused on the optimization of the Relay Transformation Matrix (RTM) and the duty cycle in a two-hop amplify-and-forward MIMO relay channel. The contributions extend earlier results from the literature. The seminal work by Tang and Hua [9] provided the solution of the optimization problem with the RCSAR as objective function for a pure relay channel (without direct link). The authors emphasized that the relay channel with a direct link case was an open problem at the time and to the author's knowledge it remained so until now. The work by Shariat and Gazor [10] established the interest in the complete relay channel but focused on the OSTBC-RCSAR only. Though the OSTBC-optimized RTM provides good results in terms of RCSAR in many cases, it remains a suboptimal approach and may lead sometimes to considerable performance degradation (see Fig. 2). Moreover, reference [10] imposed some conditions on the number of antennas of the relay channel limiting the generality of the results. These limitations are overcome in this work which does not assume any conditions on the channel matrices' ranks and on the number of antennas.

The optimum RTM has been derived in Theorems 1 and 2 for the RCSAR and OSTBC-RCSAR, respectively, by different simplified convex optimization problems, whose parametric solutions have been derived in Sections III-B and III-D, respectively. The KKT equations corresponding to the relevant optimization problems have been solved and used to provide parametric expressions of the average power constraint and the RCSAR as depending only on a single parameter. The solution recalls the structure of *water-filling* equations.

Simulation results have been presented to compare the RCSAR achieved by the optimum RTM and by naive amplify-and-forward. It is shown that the RCSAR advantage due to RTM optimization decreases as the SNR increases but it is still sizable for practical SNR values. To assess the effectiveness of a MIMO relay on an existing 2×2 MIMO link we compared different simulation scenarios corresponding to increasing numbers of relay antennas. For example, we showed in Section IV-C that RCSAR increases from 7.1 bit/s/Hz (w/o relay) to 9.9, 11.4, and 13.0 bit/s/Hz, by using a relay with $2, 4$, and 8 antennas, respectively.

Finally, the analytic approach lends itself to the optimization of the duty cycle, i.e., the fraction of time-frequency resources to be dedicated to direct transmission or relaying. In a numerical example, we have seen that for low relay-to-destination SNR, it is convenient not using relaying. The opposite holds for high relay-to-destination SNR. Intermediate values require duty cycle optimization to maximize the achievable rate.

VI. Acknowledgment

The author would like to thank the Associate Editor and the anonymous Reviewers for their useful suggestions that helped him to improve the quality of the submitted manuscript.

Appendix A
Proof of Theorem 1

Proof: We will use the following linear algebra identity:

$$\boldsymbol{K}^{\mathsf{H}}(\boldsymbol{I}+\boldsymbol{K}\boldsymbol{K}^{\mathsf{H}})^{-1}\boldsymbol{K} = \boldsymbol{K}^{\mathsf{H}}\boldsymbol{K}(\boldsymbol{I}+\boldsymbol{K}^{\mathsf{H}}\boldsymbol{K})^{-1} = \boldsymbol{I}-(\boldsymbol{I}+\boldsymbol{K}^{\mathsf{H}}\boldsymbol{K})^{-1}. \quad (35)$$

Setting $\boldsymbol{K}=\boldsymbol{H}_2\boldsymbol{X}$ in (35), we can rewrite the part of the RCSAR (7) depending on the RTM $\boldsymbol{X}$ as follows:

$$\begin{aligned}&\log_2\det\Big\{\boldsymbol{I}_t+\frac{P_1}{\theta t}\Big[\boldsymbol{H}_0^{\mathsf{H}}\boldsymbol{H}_0+\boldsymbol{H}_1^{\mathsf{H}}\boldsymbol{X}^{\mathsf{H}}\boldsymbol{H}_2^{\mathsf{H}}\\ &\qquad(\boldsymbol{I}_r+\boldsymbol{H}_2\boldsymbol{X}\boldsymbol{X}^{\mathsf{H}}\boldsymbol{H}_2^{\mathsf{H}})^{-1}\boldsymbol{H}_2\boldsymbol{X}\boldsymbol{H}_1\Big]\Big\}\\ &=\log_2\det\Big\{\boldsymbol{I}_t+\frac{P_1}{\theta t}(\boldsymbol{H}_0^{\mathsf{H}}\boldsymbol{H}_0+\boldsymbol{H}_1^{\mathsf{H}}\boldsymbol{H}_1)\\ &\qquad-\frac{P_1}{\theta t}\boldsymbol{H}_1^{\mathsf{H}}(\boldsymbol{I}_s+\boldsymbol{X}^{\mathsf{H}}\boldsymbol{H}_2^{\mathsf{H}}\boldsymbol{H}_2\boldsymbol{X})^{-1}\boldsymbol{H}_1\Big\}. \quad (36)\end{aligned}$$

According to the definitions in Section III, the optimum RTM $\boldsymbol{X}$ maximizes the RCSAR from eq. (7), under the constraint of eq. (8). Subtracting from eq. (36) the term

$$\log_2\det\Big\{\boldsymbol{I}_t+\frac{P_1}{\theta t}(\boldsymbol{H}_0^{\mathsf{H}}\boldsymbol{H}_0+\boldsymbol{H}_1^{\mathsf{H}}\boldsymbol{H}_1)\Big\}, \quad (37)$$

independent of $\boldsymbol{X}$, we can see that the optimum RTM is found by solving the optimization problem:

$$\max_{\boldsymbol{X}} \quad \det[\boldsymbol{I}_t-\boldsymbol{A}(\boldsymbol{I}_s+\boldsymbol{X}^{\mathsf{H}}\boldsymbol{B}\boldsymbol{X})^{-1}] \quad (38)$$

$$\text{s.t.} \quad \mathrm{tr}(\boldsymbol{X}\boldsymbol{C}\boldsymbol{X}^{\mathsf{H}})\le\frac{P_2}{\bar{\theta}} \quad (39)$$

where we defined the matrices $\boldsymbol{A},\boldsymbol{B},\boldsymbol{C}$ as in eqs. (11) and (12) (reported hereafter for easy reference):

$$\boldsymbol{A}\triangleq\boldsymbol{H}_1\Big(\frac{\theta t}{P_1}\boldsymbol{I}_t+\boldsymbol{H}_0^{\mathsf{H}}\boldsymbol{H}_0+\boldsymbol{H}_1^{\mathsf{H}}\boldsymbol{H}_1\Big)^{-1}\boldsymbol{H}_1^{\mathsf{H}} \quad (11)$$

$$\boldsymbol{B}\triangleq\boldsymbol{H}_2^{\mathsf{H}}\boldsymbol{H}_2,\qquad \boldsymbol{C}\triangleq\boldsymbol{I}_s+\frac{P_1}{\theta t}\boldsymbol{H}_1\boldsymbol{H}_1^{\mathsf{H}} \quad (12)$$

Now, consider the following UD's:

$$\boldsymbol{A}=\boldsymbol{U}_A\boldsymbol{\Lambda}_A\boldsymbol{U}_A^{\mathsf{H}} \quad (40)$$

$$\boldsymbol{X}^{\mathsf{H}}\boldsymbol{B}\boldsymbol{X}=\boldsymbol{U}\boldsymbol{\Lambda}\boldsymbol{U}^{\mathsf{H}} \quad (41)$$

The objective function can be upper bounded as follows:

$$\begin{aligned}&\det[\boldsymbol{I}_s-\boldsymbol{A}(\boldsymbol{I}_s+\boldsymbol{X}^{\mathsf{H}}\boldsymbol{B}\boldsymbol{X})^{-1}]\\ &=\det[\boldsymbol{I}_s-\boldsymbol{U}_A\boldsymbol{\Lambda}_A\boldsymbol{U}_A^{\mathsf{H}}(\boldsymbol{I}_s+\boldsymbol{U}\boldsymbol{\Lambda}\boldsymbol{U}^{\mathsf{H}})^{-1}]\\ &=\det[\boldsymbol{I}_s-\boldsymbol{U}^{\mathsf{H}}\boldsymbol{U}_A\boldsymbol{\Lambda}_A\boldsymbol{U}_A^{\mathsf{H}}\boldsymbol{U}(\boldsymbol{I}_s+\boldsymbol{\Lambda})^{-1}]\\ &=\det[\boldsymbol{I}_s-\boldsymbol{Q}\boldsymbol{\Lambda}_A\boldsymbol{Q}^{\mathsf{H}}(\boldsymbol{I}_s+\boldsymbol{\Lambda})^{-1}]\\ &=\frac{\det(\boldsymbol{I}_s+\boldsymbol{\Lambda}-\boldsymbol{Q}\boldsymbol{\Lambda}_A\boldsymbol{Q}^{\mathsf{H}})}{\det(\boldsymbol{I}_s+\boldsymbol{\Lambda})}\\ &\le\prod_{i=1}^{s}\Big\{1-\frac{(\boldsymbol{\Lambda}_A)_{i,i}}{1+(\boldsymbol{\Lambda})_{i,i}}\Big\}. \quad (42)\end{aligned}$$

Here, we set $\boldsymbol{Q}\triangleq\boldsymbol{U}^{\mathsf{H}}\boldsymbol{U}_A$ (i.e., a unitary matrix) and then we applied [21, eq.(2)] after noticing that both $\boldsymbol{\Lambda}$ and $\boldsymbol{I}_s-\boldsymbol{Q}\boldsymbol{\Lambda}_A\boldsymbol{Q}^{\mathsf{H}}$ are Hermitian positive semidefinite matrices and the nondecreasingly ordered eigenvalues of $\boldsymbol{I}_s-\boldsymbol{Q}\boldsymbol{\Lambda}_A\boldsymbol{Q}^{\mathsf{H}}$ are $1-(\boldsymbol{\Lambda}_A)_{i,i}, i=1,\ldots,s$. The upper bound is attained by setting $\boldsymbol{Q}=\boldsymbol{I}_s$. Hence, $\boldsymbol{U}=\boldsymbol{U}_A$.

To find an expression of the RTM $\boldsymbol{X}$, we notice that both sides of (41) have the same rank:

$$\rho\triangleq\mathrm{rank}(\boldsymbol{X}^{\mathsf{H}}\boldsymbol{B}\boldsymbol{X})=\mathrm{rank}(\boldsymbol{U}_A\boldsymbol{\Lambda}\boldsymbol{U}_A^{\mathsf{H}})\le\min(s,u,r). \quad (43)$$

If $\rho_B\triangleq\mathrm{rank}(\boldsymbol{B})$, then $\rho_B\ge\rho$, and we have the following "thin" UD's:

$$\boldsymbol{B}=\underbrace{\widetilde{\boldsymbol{U}}_B\widetilde{\boldsymbol{\Lambda}}_B\widetilde{\boldsymbol{U}}_B^{\mathsf{H}}}_{u\times\rho_B\times\rho_B\times u}\qquad \boldsymbol{U}_A\boldsymbol{\Lambda}\boldsymbol{U}_A^{\boldsymbol{H}}=\underbrace{\widetilde{\boldsymbol{U}}_A\widetilde{\boldsymbol{\Lambda}}\widetilde{\boldsymbol{U}}_A^{\mathsf{H}}}_{s\times\rho_B\times\rho_B\times s} \quad (44)$$

where $\widetilde{\boldsymbol{U}}_B^{\mathsf{H}}\widetilde{\boldsymbol{U}}_B=\widetilde{\boldsymbol{U}}_A^{\mathsf{H}}\widetilde{\boldsymbol{U}}_A=\boldsymbol{I}_{\rho_B}$, $\widetilde{\boldsymbol{\Lambda}}_B$ is the diagonal submatrix of $\boldsymbol{\Lambda}_B$ with the positive elements, and $\widetilde{\boldsymbol{\Lambda}}$ is the *unknown* diagonal submatrix of $\boldsymbol{\Lambda}$ with nonnegative elements while the other elements of $\boldsymbol{\Lambda}$ (if any) are all equal to 0. Thus, eq. (41) is satisfied by setting

$$\boldsymbol{X}=\widetilde{\boldsymbol{U}}_B\widetilde{\boldsymbol{\Lambda}}_B^{-1/2}\widetilde{\boldsymbol{\Lambda}}^{1/2}\widetilde{\boldsymbol{U}}_A^{\mathsf{H}}. \quad (45)$$

Remark A.1 Notice that the maximum in (42) is attained regardless of any constraint by the matrix $\boldsymbol{X}$ with the structure given in (45). For every pair of Hermitian positive semidefinite matrices $\boldsymbol{A}$ and $\boldsymbol{B}$, the matrix defined in (45) maximizes

$$\det[\boldsymbol{I}_t-\boldsymbol{A}(\boldsymbol{I}_s+\boldsymbol{X}^{\mathsf{H}}\boldsymbol{B}\boldsymbol{X})^{-1}], \quad (46)$$

and thus the RCSAR (36). The structure (45) contains ρ free parameters as the diagonal elements of $\widetilde{\boldsymbol{\Lambda}}$. The relay power constraint is introduced in the following optimization problem.

Now, we have to choose $\widetilde{\boldsymbol{\Lambda}}$ in order to $i)$ maximize the upper bound in (42), namely,

$$\prod_{i=1}^{s}\Big\{1-\frac{(\boldsymbol{\Lambda}_A)_{i,i}}{1+(\boldsymbol{\Lambda})_{i,i}}\Big\},$$

and $ii)$ satisfy the relay power constraint (8), namely,

$$\mathrm{tr}(\boldsymbol{X}\boldsymbol{C}\boldsymbol{X}^{\mathsf{H}})\le\frac{P_2}{\bar{\theta}}, \quad (47)$$

with $\boldsymbol{C}$ defined in eq. (12). Since

$$\begin{aligned}\mathrm{tr}(\boldsymbol{X}\boldsymbol{C}\boldsymbol{X}^{\mathsf{H}})&=\mathrm{tr}(\widetilde{\boldsymbol{U}}_B\widetilde{\boldsymbol{\Lambda}}_B^{-1/2}\widetilde{\boldsymbol{\Lambda}}^{1/2}\widetilde{\boldsymbol{U}}_A^{\mathsf{H}}\boldsymbol{C}\widetilde{\boldsymbol{U}}_A\widetilde{\boldsymbol{\Lambda}}^{1/2}\widetilde{\boldsymbol{\Lambda}}_B^{-1/2}\widetilde{\boldsymbol{U}}_B^{\mathsf{H}})\\ &=\mathrm{tr}(\widetilde{\boldsymbol{\Lambda}}_B^{-1}\widetilde{\boldsymbol{\Lambda}}\widetilde{\boldsymbol{U}}_A^{\mathsf{H}}\boldsymbol{C}\widetilde{\boldsymbol{U}}_A), \quad (48)\end{aligned}$$

we can write the power constraint equation as

$$\sum_{i=1}^{\rho}\frac{(\widetilde{\boldsymbol{U}}_A^{\mathsf{H}}\boldsymbol{C}\widetilde{\boldsymbol{U}}_A)_{i,i}}{(\widetilde{\boldsymbol{\Lambda}}_B)_{i,i}}(\boldsymbol{\Lambda})_{i,i}=\frac{P_2}{\bar{\theta}}. \quad (49)$$

Notice that the inequality in (8) is turned into an equality since a possibly optimum solution $\boldsymbol{\Lambda}_0$ such that

$$\sum_{i=1}^{\rho}\frac{(\widetilde{\boldsymbol{U}}_A^{\mathsf{H}}\boldsymbol{C}\widetilde{\boldsymbol{U}}_A)_{i,i}}{(\widetilde{\boldsymbol{\Lambda}}_B)_{i,i}}(\boldsymbol{\Lambda}_0)_{i,i}=\rho\frac{P_2}{\bar{\theta}}<\frac{P_2}{\bar{\theta}}, \quad (50)$$

for some $0<\rho<1$, cannot be optimum since $\rho^{-1}\boldsymbol{\Lambda}_0$ would increase all the factors in the upper bound in (42) since

$$1-\frac{(\boldsymbol{\Lambda}_A)_{i,i}}{1+\rho^{-1}(\boldsymbol{\Lambda}_0)_{i,i}}>1-\frac{(\boldsymbol{\Lambda}_A)_{i,i}}{1+(\boldsymbol{\Lambda}_0)_{i,i}}. \quad (51)$$

The detailed solution of this optimization problem is reported in the following App. B and completes the proof of Theorem 1. ■

Appendix B
Parametric solution of optimization problem (14)

From the statement of the optimization problem reported in eq. (14) of Theorem 1, we derive the Lagrangian function of the problem as follows:

$$\mathcal{L}(\boldsymbol{x},\lambda_0,\lambda_1,\ldots,\lambda_\rho) = -\sum_{i=1}^{\rho}\ln\left\{1-\frac{\alpha_i}{1+x_i}\right\} + \lambda_0\left(\boldsymbol{\beta}^{\mathsf{T}}\boldsymbol{x}-\frac{P_2}{\bar{\theta}}\right) - \sum_{i=1}^{\rho}\lambda_i x_i. \tag{52}$$

where $0<\alpha_i<1, \beta_i>0$ and $\lambda_i, i=0,\ldots,\rho$, are the Lagrange multipliers [22]. Here, we did not consider the constraints $x_1 \geq x_2 \geq \cdots \geq x_\rho$ since, by Lemma E.1, these constraint are automatically satisfied by any nonnegative solution ($x_i \geq 0, i=1,\ldots,\rho$). In fact, otherwise, a permutation of the variables would lead to a further decrease of the objective function. Thus, we can save the extra effort that would be required. The KKT equations are obtained according to [22, Sec. 5.5.3]. First, we take the partial derivatives of the Lagrangian function with respect to the variables x_i, for $i=1,\ldots,\rho$:

$$\frac{\partial\mathcal{L}}{\partial x_i} = \frac{1}{1+x_i} - \frac{1}{1-\alpha_i+x_i} + \lambda_0\beta_i - \lambda_i \tag{53}$$

Then, we have the following KKT equations:

$$\begin{cases} \boldsymbol{\beta}^{\mathsf{T}}\boldsymbol{x}-\dfrac{P_2}{\bar{\theta}} & \leq 0 \\ \lambda_0\left(\boldsymbol{\beta}^{\mathsf{T}}\boldsymbol{x}-\dfrac{P_2}{\bar{\theta}}\right) & = 0 \\ \lambda_0 & \geq 0 \\ -x_i & \leq 0 \quad i=1,\ldots,\rho \\ \lambda_i x_i & = 0 \quad i=1,\ldots,\rho \\ \lambda_i & \geq 0 \quad i=1,\ldots,\rho \\ \dfrac{\partial\mathcal{L}}{\partial x_i} & = 0 \quad i=1,\ldots,\rho \end{cases} \tag{54}$$

We can see that the objective function

$$f(\boldsymbol{x}) \triangleq -\sum_{i=1}^{\rho}\ln\left\{1-\frac{\alpha_i}{1+x_i}\right\} \tag{55}$$

is convex for $\boldsymbol{x}\geq\boldsymbol{0}$ because

$$\frac{\partial^2 f}{\partial x_i^2} = \frac{\alpha_i(2-\alpha_i+2x_i)}{(1+x_i)^2(1-\alpha_i+x_i)^2} \geq 0. \tag{56}$$

The mixed derivatives $\partial^2 f/(\partial x_i \partial x_j) = 0$ for all $i \neq j$. Therefore, we have a convex optimization problem. We can see that Slater's condition is satisfied, so that the KKT equations are sufficient for optimality.

The constraint $\boldsymbol{\beta}^{\mathsf{T}}\boldsymbol{x}-\frac{P_2}{\bar{\theta}}\leq 0$ is achieved with equality since $f(\boldsymbol{x})$ is decreasing with every x_i. Therefore, we have $\lambda_0 \geq 0$.

Finally, we obtain from the gradient equations:

$$\frac{1}{1-\alpha_i+x_i} - \frac{1}{1+x_i} = \lambda_0\beta_i - \lambda_i, \quad i=1,\ldots,\rho. \tag{57}$$

For a given $\lambda_0 \geq 0$, recalling that $\lambda_i \geq 0, x_i \geq 0, \lambda_i x_i = 0$, there are two possible cases

- $\lambda_i = 0$, which implies that the equation is equivalent to
$$x_i^2 + (2-\alpha_i)x_i + 1 - \alpha_i - \frac{\alpha_i}{\lambda_0\beta_i} = 0 \tag{58}$$
Since $0<\alpha_i<1$, a solution $x_i>0$ exists only if
$$1-\alpha_i-\frac{\alpha_i}{\lambda_0\beta_i} < 0 \Longrightarrow \lambda_0 < \frac{\alpha_i}{(1-\alpha_i)\beta_i} \tag{59}$$
and is given by
$$x_i = \frac{\alpha_i}{2} - 1 + \sqrt{\frac{\alpha_i^2}{4}+\frac{\alpha_i}{\lambda_0\beta_i}}. \tag{60}$$
- $\lambda_i > 0$, which implies that one root of (58) must be equal to 0 to satisfy the KKT condition $\lambda_i x_i = 0$. In turn, this implies that
$$1-\alpha_i-\frac{\alpha_i}{\lambda_0\beta_i-\lambda_i} = 0 \tag{61}$$
and hence
$$\lambda_0 = \frac{\alpha_i}{(1-\alpha_i)\beta_i} + \frac{\lambda_i}{\beta_i} > \frac{\alpha_i}{(1-\alpha_i)\beta_i}, \tag{62}$$
so that
$$\frac{\alpha_i}{2} - 1 + \sqrt{\frac{\alpha_i^2}{4}+\frac{\alpha_i}{\lambda_0\beta_i}} < \frac{\alpha_i}{2} - 1 + \sqrt{\frac{\alpha_i^2}{4}+1-\alpha_i} = 0 \tag{63}$$

Summarizing, we can write the solution in all cases as

$$x_i = \left\{\frac{\alpha_i}{2} - 1 + \sqrt{\frac{\alpha_i^2}{4}+\frac{\alpha_i}{\lambda_0\beta_i}}\right\}_+ \tag{64}$$

Thus, the unknown $\lambda_0 \geq 0$ can be found by solving the nonlinear equation

$$\frac{P_2}{\bar{\theta}} = \sum_{i=1}^{\rho}\beta_i\left\{\frac{\alpha_i}{2} - 1 + \sqrt{\frac{\alpha_i^2}{4}+\frac{\alpha_i}{\lambda_0\beta_i}}\right\}_+ \tag{65}$$

A unique solution always exists because the rhs is a monotonically decreasing function of λ_0, which is identically equal to 0 when $\lambda_0 \geq \max_{1\leq i\leq\rho}\frac{\alpha_i}{(1-\alpha_i)\beta_i}$. Setting $\xi \triangleq 1/\lambda_0$ yields the parametric solution reported in eqs. (16) to (18).

Appendix C
Proof of Theorem 2

Proof: We proceed, as in the proof of Theorem 1 of Appendix A, to apply the identity (35) to the trace argument of (19). We obtain:

$$\boldsymbol{H}_1^{\mathsf{H}}\boldsymbol{X}^{\mathsf{H}}\boldsymbol{H}_2^{\mathsf{H}}(\boldsymbol{I}_r+\boldsymbol{H}_2\boldsymbol{X}\boldsymbol{X}^{\mathsf{H}}\boldsymbol{H}_2^{\mathsf{H}})^{-1}\boldsymbol{H}_2\boldsymbol{X}\boldsymbol{H}_1 \tag{66}$$
$$= \boldsymbol{H}_1^{\mathsf{H}}\boldsymbol{H}_1 - \boldsymbol{H}_1^{\mathsf{H}}(\boldsymbol{I}_s+\boldsymbol{X}^{\mathsf{H}}\boldsymbol{H}_2^{\mathsf{H}}\boldsymbol{H}_2\boldsymbol{X})^{-1}\boldsymbol{H}_1 \tag{67}$$

After defining the matrices $\check{\boldsymbol{A}}, \check{\boldsymbol{B}}, \boldsymbol{C}$ as in (22), we get the following expression for the optimization problem to maximize the OSTBC-RCSAR (19):

$$\begin{cases} \min\limits_{\boldsymbol{X}} & \mathrm{tr}\{\check{\boldsymbol{A}}(\boldsymbol{I}_s+\boldsymbol{X}^{\mathsf{H}}\check{\boldsymbol{B}}\boldsymbol{X})^{-1}\} \\ \text{s.t.} & \mathrm{tr}\{\boldsymbol{X}\boldsymbol{C}\boldsymbol{X}^{\mathsf{H}}\} \leq \dfrac{P_2}{\bar{\theta}} \end{cases} \tag{68}$$

Calculating the UD's

$$\check{\boldsymbol{A}} = \check{\boldsymbol{U}}_A\check{\boldsymbol{\Lambda}}_A\check{\boldsymbol{U}}_A^{\mathsf{H}} \qquad \boldsymbol{X}^{\mathsf{H}}\check{\boldsymbol{B}}\boldsymbol{X} = \check{\boldsymbol{U}}\check{\boldsymbol{\Lambda}}\check{\boldsymbol{U}}^{\mathsf{H}} \tag{69}$$

and defining the matrix $\check{\boldsymbol{Q}} \triangleq \check{\boldsymbol{U}}^{\mathsf{H}}\check{\boldsymbol{U}}_A$, we can rewrite optimization problem (68) as

$$\begin{cases} \min\limits_{\boldsymbol{X}} & \mathrm{tr}\{(\boldsymbol{I}+\check{\boldsymbol{\Lambda}})^{-1}\check{\boldsymbol{Q}}\check{\boldsymbol{\Lambda}}_A\check{\boldsymbol{Q}}^{\mathsf{H}}\} \\ \text{s.t.} & \mathrm{tr}\{\boldsymbol{X}\boldsymbol{C}\boldsymbol{X}^{\mathsf{H}}\} \leq \dfrac{P_2}{\bar{\theta}} \end{cases} \tag{70}$$

The objective function can be written as

$$\mathrm{tr}\{(\boldsymbol{I}+\check{\boldsymbol{\Lambda}})^{-1}\check{\boldsymbol{Q}}\check{\boldsymbol{\Lambda}}_A\check{\boldsymbol{Q}}^{\mathsf{H}}\} = \sum_{i=1}^{s}\sum_{j=1}^{s}\frac{|(\check{\boldsymbol{Q}})_{i,j}|^2(\check{\boldsymbol{\Lambda}}_A)_{j,j}}{1+(\check{\boldsymbol{\Lambda}})_{i,i}} \tag{71}$$

$$= \tilde{\boldsymbol{\lambda}}^{\mathsf{T}}\widetilde{\boldsymbol{Q}}\boldsymbol{\lambda}_A \tag{72}$$

where we defined the column vectors $\tilde{\boldsymbol{\lambda}}, \boldsymbol{\lambda}_A$ and the matrix $\widetilde{\boldsymbol{Q}}$ by

$$(\tilde{\boldsymbol{\lambda}})_i \triangleq \frac{1}{1+(\check{\boldsymbol{\Lambda}})_{i,i}} \qquad i=1,\ldots,s \tag{73}$$

$$(\boldsymbol{\lambda}_A)_j \triangleq (\check{\boldsymbol{\Lambda}}_A)_{j,j} \qquad j=1,\ldots,s \tag{74}$$

$$(\widetilde{\boldsymbol{Q}})_{i,j} \triangleq |(\check{\boldsymbol{Q}})_{i,j}|^2 \qquad i,j=1,\ldots,s \tag{75}$$

Since $\boldsymbol{Q}$ is a unitary matrix, $\widetilde{\boldsymbol{Q}}$ is a *doubly stochastic* matrix and, by Birkhoff's theorem [17, Th.8.7.2], it can be written as the weighted sum of a certain number of permutation matrices:

$$\widetilde{\boldsymbol{Q}} = \sum_{\ell=1}^{N} w_\ell \boldsymbol{\Pi}_\ell \tag{76}$$

with $N \leq s^2-s+1$, $w_\ell \geq 0, \ell=1,\ldots,N$, and $\sum_{\ell=1}^{N} w_\ell = 1$. Thus,

$$\begin{aligned}\min_{\check{\boldsymbol{Q}}:\check{\boldsymbol{Q}}\check{\boldsymbol{Q}}^{\mathsf{H}}=\boldsymbol{I}} \mathrm{tr}\{(\boldsymbol{I}+\check{\boldsymbol{\Lambda}})^{-1}\check{\boldsymbol{Q}}\check{\boldsymbol{\Lambda}}_A\check{\boldsymbol{Q}}^{\mathsf{H}}\} &= \sum_{\ell=1}^{N} w_\ell \tilde{\boldsymbol{\lambda}}^{\mathsf{T}}\boldsymbol{\Pi}_\ell\boldsymbol{\lambda}_A \\ &= \min_{1\leq\ell\leq N} \tilde{\boldsymbol{\lambda}}^{\mathsf{T}}\boldsymbol{\Pi}_\ell\boldsymbol{\lambda}_A \\ &= \min_{1\leq\ell\leq N}\sum_{i=1}^{s}\frac{(\check{\boldsymbol{\Lambda}}_A)_{\pi_\ell(i),\pi_\ell(i)}}{1+(\check{\boldsymbol{\Lambda}})_{i,i}}\end{aligned} \tag{77}$$

where π_ℓ is the permutation associated to the permutation matrix $\boldsymbol{\Pi}_\ell$ defined by

$$(\boldsymbol{\Pi}_\ell)_{i,j} = \delta_{\pi_\ell(i),j} \tag{78}$$

where $\delta_{a,b} = 1$ if $a=b$ and 0 otherwise (Kronecker delta function). The optimum permutation can be found by applying the lower bound of Lemma E.1 from Appendix E:

$$\min_{\check{\boldsymbol{Q}}:\check{\boldsymbol{Q}}\check{\boldsymbol{Q}}^{\mathsf{H}}=\boldsymbol{I}} \mathrm{tr}\{(\boldsymbol{I}+\check{\boldsymbol{\Lambda}})^{-1}\check{\boldsymbol{Q}}\check{\boldsymbol{\Lambda}}_A\check{\boldsymbol{Q}}^{\mathsf{H}}\} = \sum_{i=1}^{\rho_A}\frac{(\check{\boldsymbol{\Lambda}}_A)_{i,i}}{1+(\check{\boldsymbol{\Lambda}})_{i,i}} \tag{79}$$

where $\rho_A \triangleq \mathrm{rank}(\check{\boldsymbol{A}}) = \mathrm{rank}(\boldsymbol{H}_1) \leq \min(t,s)$. We notice that the optimum solution found above corresponds to setting $\check{\boldsymbol{Q}} = \boldsymbol{I}_s$, which implies $\check{\boldsymbol{U}} = \check{\boldsymbol{U}}_A$. We also have to take into account the additional constraint stemming from the inequality

$$\rho \triangleq \mathrm{rank}(\check{\boldsymbol{\Lambda}}) \leq \min(\rho_B, s) \tag{80}$$

where $\rho_B \triangleq \mathrm{rank}(\check{\boldsymbol{B}}) = \mathrm{rank}(\boldsymbol{H}_2) \leq \min(r,u)$. Using the "thin" UD

$$\check{\boldsymbol{B}} = \underbrace{\widetilde{\boldsymbol{U}}_B\widetilde{\boldsymbol{\Lambda}}_B\widetilde{\boldsymbol{U}}_B^{\mathsf{H}}}_{u\times\rho_B\times\rho_B\times u}, \tag{81}$$

eq. (41) is satisfied by setting

$$\boldsymbol{X} = \widetilde{\boldsymbol{U}}_B\widetilde{\boldsymbol{\Lambda}}_B^{-1/2}\widetilde{\boldsymbol{\Lambda}}^{1/2}\widetilde{\boldsymbol{U}}_A^{\mathsf{H}}, \tag{82}$$

where $\widetilde{\boldsymbol{U}}_A$ is obtained by taking the first ρ columns of $\boldsymbol{U}_A$, and the relay power constraint (8) becomes

$$\sum_{i=1}^{\rho}\frac{(\widetilde{\boldsymbol{U}}_A^{\mathsf{H}}\boldsymbol{C}\widetilde{\boldsymbol{U}}_A)_{i,i}}{(\widetilde{\boldsymbol{\Lambda}}_B)_{i,i}}(\check{\boldsymbol{\Lambda}})_{i,i} \leq \frac{P_2}{\bar{\theta}}, \tag{83}$$

which completes the proof of Theorem 2. ■

Appendix D
Parametric solution of optimization problem (23)

We proceed as in App. B with the Lagrangian

$$\mathcal{L}(\boldsymbol{x},\lambda_0,\lambda_1,\ldots,\lambda_\rho) = \sum_{i=1}^{\rho}\frac{\alpha_i}{1+x_i} + \lambda_0\left(\boldsymbol{\beta}^{\mathsf{T}}\boldsymbol{x} - \frac{P_2}{\bar{\theta}}\right) - \sum_{i=1}^{\rho}\lambda_i x_i. \tag{84}$$

The Lagrangian derivatives are

$$\frac{\partial\mathcal{L}}{\partial x_i} = -\frac{\alpha_i}{(1+x_i)^2} + \lambda_0\beta_i - \lambda_i \tag{85}$$

The KKT equations remain the same as (54) from App. B. The objective function is

$$f(\boldsymbol{x}) \triangleq \sum_{i=1}^{\rho}\frac{\alpha_i}{1+x_i}, \tag{86}$$

which is plainly convex for $\boldsymbol{x} \geq \boldsymbol{0}$ so that we have a convex optimization problem. Slater's condition is satisfied so that the KKT equations are sufficient for optimality. Again, $\boldsymbol{\beta}^{\mathsf{T}}\boldsymbol{x} - \frac{P_2}{\bar{\theta}} \leq 0$ is achieved with equality since $f(\boldsymbol{x})$ is decreasing with every x_i, so that $\lambda_0 \geq 0$. The gradient equations are:

$$\frac{\alpha_i}{(1+x_i)^2} = \lambda_0\beta_i - \lambda_i, \quad i=1,\ldots,\rho. \tag{87}$$

For a given $\lambda_0 \geq 0$, recalling that $\lambda_i \geq 0, x_i \geq 0, \lambda_i x_i = 0$, we can get the solution:

$$x_i = \left\{\xi\sqrt{\frac{\alpha_i}{\beta_i}} - 1\right\}_+ \tag{88}$$

where $\xi \triangleq \lambda_0^{-1/2}$ and $\{\cdot\}_+ \triangleq \max(0,\cdot)$. Thus, the unknown $\xi > 0$ can be found by solving the nonlinear equation[6]

$$\frac{P_2}{\bar{\theta}} = \sum_{i=1}^{\rho}(\xi\sqrt{\alpha_i\beta_i} - \beta_i)\cdot 1_{\xi>\sqrt{\beta_i/\alpha_i}}$$

A unique solution always exists because the rhs is a monotonically increasing function of ξ for

$$\xi \geq \min_{1\leq i\leq\rho}\sqrt{\frac{\beta_i}{\alpha_i}}.$$

[6] $1_{\mathcal{A}} = 1$ when $\mathcal{A}$ is true and 0 otherwise.

APPENDIX E
SEQUENCE PRODUCT SUM LEMMA

Lemma E.1 *Given any two real nonnegative nonincreasing sequences $\alpha_i, \beta_i, i = 1, \ldots, n$ such that $\alpha_i \geq \alpha_{i+1}$ and $\beta_i \geq \beta_{i+1}$, for $i = 1, \ldots, n-1$, we have, for every permutation π, the following inequality:*

$$\sum_{i=1}^{n} \alpha_i \beta_{n+1-i} \leq \sum_{i=1}^{n} \alpha_i \beta_{\pi(i)} \leq \sum_{i=1}^{n} \alpha_i \beta_i. \tag{89}$$

Proof: Since every permutation $\pi \in S_n$ can be expressed as a product of disjoint *cycles* [23, Sec. III.70], we have to prove the inequalities only when π is a cycle and then apply it to any $\pi \in S_n$ after proper relabeling of the indexes. Let us assume, w.l.o.g., that $\pi = (1, \ldots, n)$, i.e., the permutation $1 \mapsto 2 \mapsto 3 \mapsto \cdots \mapsto n \mapsto 1$. For the upper bound, we have to show that

$$\alpha_1(\beta_1 - \beta_2) + \alpha_2(\beta_2 - \beta_3) + \cdots + \alpha_n(\beta_n - \beta_1) \geq 0.$$

The above inequality stems from the following:

$$\begin{aligned}
&\alpha_1(\beta_1 - \beta_2) + \alpha_2(\beta_2 - \beta_3) + \cdots + \alpha_n(\beta_n - \beta_1) \\
&= (\alpha_1 - \alpha_n)(\beta_1 - \beta_2) + \cdots + (\alpha_{n-1} - \alpha_n)(\beta_{n-1} - \beta_n) \\
&\geq 0,
\end{aligned}$$

since $\alpha_i - \alpha_n \geq 0$ and $\beta_i - \beta_{i+1} \geq 0$ for every $i = 1, \ldots, n-1$.

Similary, for the lower bound, we have to show that

$$\begin{aligned}
&\alpha_1(\beta_n - \beta_{n-1}) + \alpha_2(\beta_{n-1} - \beta_{n-2}) \\
&\qquad + \cdots + \alpha_n(\beta_1 - \beta_n) \leq 0.
\end{aligned}$$

The above inequality stems from the following:

$$\begin{aligned}
&\alpha_1(\beta_n - \beta_{n-1}) + \alpha_2(\beta_{n-1} - \beta_{n-2}) + \cdots + \alpha_n(\beta_1 - \beta_n) \\
&= (\alpha_1 - \alpha_n)(\beta_n - \beta_{n-1}) + \cdots + (\alpha_{n-1} - \alpha_n)(\beta_2 - \beta_1) \\
&\leq 0,
\end{aligned}$$

since $\alpha_i - \alpha_n \geq 0$ and $\beta_i - \beta_{i-1} \leq 0$ for every $i = 1, \ldots, n-1$. ■

REFERENCES

[1] G. Taricco, "Information Rate Optimization for Joint Relay and Link in Non-Regenerative MIMO Channels," *IEEE ISIT 2021*.

[2] E.C. Van Der Meulen, "Three terminal communication channels," *Adv. Appl. Prob.*, vol. 3, pp. 120–154, 1971.

[3] T.M. Cover and A.A. El Gamal, "Capacity theorems for the relay channel," *IEEE Trans. Inf. Theory*, vol. 25, no. 5, pp. 572–584, Sept. 1979.

[4] A. Sendonaris, E. Erkip, and B. Aazhang, "User cooperation diversity – part I and part II," *IEEE Trans. Commun.*, vol. 51, no. 11, pp. 1927–1948, Nov. 2003.

[5] R.U. Nabar, H. Bolcskei, and F.W. Kneubuhler, "Fading relay channels: performance limits and space-time signal design," *IEEE J. Sel. Areas Commun.*, vol. 22, no. 6, pp. 1099–1109, Aug. 2004.

[6] J.N. Laneman, D.N.C. Tse, and G.W. Wornell, "Cooperative diversity in wireless networks: efficient protocols and outage behavior," *IEEE Trans. Inf. Theory*, vol. 50, no. 12, pp. 3062–3080, Dec. 2004.

[7] A. Host-Madsen and J. Zhang, "Capacity bounds and power allocation for wireless relay channel," *IEEE Trans. Inf. Theory*, vol. 51, no. 6, pp. 2020–2040, June 2005.

[8] B. Wang, J. Zhang, and A. Host-Madsen, "On the capacity of MIMO relay channels," *IEEE Trans. Inf. Theory*, vol. 51, no. 1, pp. 29–43, Jan. 2005.

[9] X. Tang and Y. Hua, "Optimal design of non-regenerative MIMO wireless relays," *IEEE Trans. Wireless Commun.*, vol. 6, no. 4, pp. 1398–1407, 2007.

[10] M.H. Shariat and S. Gazor, "Optimal non-regenerative linear MIMO relay for orthogonal space time codes," in *IEEE Signal Processing Letters*, vol. 21, no. 2, pp. 163–167, Feb. 2014.

[11] K.C. Lee, C.P. Li,T.Y. Wang, and H.J. Li, "Performance analysis of dual-hop amplify-and-forward systems with multiple antennas and co-channel interference," *IEEE Trans. Wireless Commun.*, vol. 13, no. 6, pp. 3070–3087, June 2014.

[12] X. Liang, Z. Ding, and C. Xiao, "On linear precoding of nonregenerative MIMO relay networks for finite-alphabet source," *IEEE Trans. Veh. Technol.*, vol. 66, no. 11, pp. 9005–9017, Nov. 2017.

[13] X. Jin and Y.-H. Kim, "The Approximate Capacity of the MIMO Relay Channel," *IEEE Transactions on Information Theory*, vol. 63, no. 2, pp. 1167-1176, Feb. 2017.

[14] X. Wu, L.P. Barnes and A. Özgür, """The Capacity of the Relay Channel": Solution to Cover's Problem in the Gaussian Case," *IEEE Transactions on Information Theory*, vol. 65, no. 1, pp. 255-275, Jan. 2019.

[15] A. El Gamal and Y.-H. Kim, *Network Information Theory*. Cambridge University Press, 2011.

[16] Yingbin Liang and V. V. Veeravalli, "Gaussian orthogonal relay channels: optimal resource allocation and capacity," *IEEE Transactions on Information Theory*, vol. 51, no. 9, pp. 3284-3289, Sept. 2005.

[17] R. Horn and C. Johnson, *Matrix Analysis (2nd ed.)*. New York: Cambridge University Press, 2013.

[18] T.M. Cover and J.A. Thomas, *Elements of Information Theory*. New York: Wiley, 2006.

[19] E.G. Larsson and P. Stoica, *Space-time Block Coding for Wireless Communications*. Cambridge University Press, 2003.

[20] I.E.Telatar, "Capacity of multi-antenna Gaussian channels," *European Trans. Telecommun.*, vol.10, no.6, pp.585–595, Nov.1999.

[21] M. Fiedler, "Bounds for the determinant of the sum of Hermitian matrices," *Proc. Amer. Math. Soc.*, vol. 30, no. 1, Sept. 1971, pp. 27–31.

[22] S. Boyd and L. Vandenberghe, *Convex Optimization*. Cambridge University Press, 2004.

[23] T. Gowers, *The Princeton Companion to Mathematics*. Princeton University Press, 2008.

Giorgio Taricco (M '91 – SM '03 – F '10) was born in Torino, Italy. He received the degree of Ingegnere Elettronico (*cum laude*) from Politecnico di Torino (Italy) in 1985. He was a researcher at CSELT (Italian Telecom Labs) from 1985 to 1987 where he was involved in the design process of the GSM mobile telephony standard (channel coding). Since 1991 he has been with the Department of Electronics and Telecommunications (DET) at Politecnico di Torino, first as an Assistant Professor and, since 2010, as a Full Professor. In 1996 he was a Research Fellow at ESA/ESTEC, The Netherlands. He participated in several committees of IEEE conferences (as Treasurer) and he has been an Associate Editor of the *IEEE Communications Letters*, the *IEEE Transactions on Information Theory*, and the *Journal on Communications and Networks*. He was also Senior Associate Editor for the *IEEE Wireless Communications Letters*.

His research interests include: information theory, error-control coding, multiuser detection, space-time coding , MIMO communications, cognitive radio networks, sensor networks, IoT satellite networks, MIMO relay channels. He has co-authored more than two hundreds papers published in international journals and international conferences, several book chapters, and two international patents. He was co-recipient of Best Paper Awards in the WPMC 2001 conference and in the *Journal of Communications and Networks (Special Issue on Coding and Signal Processing for MIMO Systems)* (2003). He has been in the ISI Highly Cited Researcher list in the category Computer Science from 2008 to 2013.